

Electrochemically Activated Catalytic Pathways of Human Metabolic Cytochrome P450s in Ultrathin Films

Sadagopan Krishnan and James F. Rusling

1 Introduction

Among many enzymes containing the heme iron porphyrin cofactor, the cyt P450s represent a unique and important class of monooxygenases for their major role in drug and xenobiotic metabolism in humans. Cyt P450s are involved in human metabolism of about 75 % of all marketed drugs and there are about 57 isoforms of cyt P450s identified in humans [1, 2]. Some of the reactions catalyzed by cyt P450 enzymes include epoxidation, carbon hydroxylation, dealkylation, heteroatom oxygenation, and group transfer [3]. The attractive features of cyt P450s include their broad substrate specificity with unusual catalytic properties in catalyzing a wide variety of reactions with exquisite stereoselectivity [4]. Despite intense research efforts, the catalytic mechanisms of cyt P450s are not understood completely [1, 3, 5]. Nevertheless, significant progress has been made in understanding the redox chemistry of human cyt P450s and successfully obtaining crystal structures of various human cyt P450 isoforms [6–9]. Although differences in substrate specificities and redox properties and cellular locations of the membranous and

S. Krishnan (✉)

Department of Chemistry, Oklahoma State University, Stillwater 74078, USA
e-mail: gopan.krishnan@okstate.edu

J.F. Rusling

Department of Chemistry, University of Connecticut, Storrs, CT 06269, USA
e-mail: james.rusling@uconn.edu

J.F. Rusling

Department of Surgery and Neag Cancer Center, University of Connecticut Health Center, Farmington 06032, USA

J.F. Rusling

Institute of Materials Science, University of Connecticut, Storrs, CT 06269, USA

J.F. Rusling

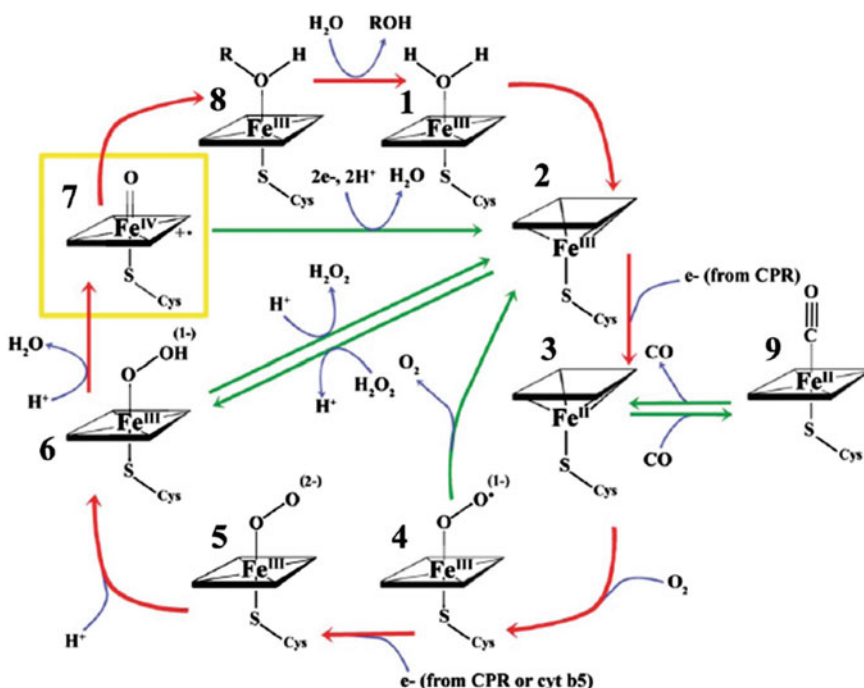
School of Chemistry, National University of Ireland at Galway, Galway, Ireland

soluble bacterial cyt P450 forms have been noticed, considerable structural similarities exist among various cyt P450 isoforms.

The purpose of this chapter is to provide an overview of the electrochemically activated catalytic and ligand binding pathways of human metabolic cyt P450s coated as ultrathin films on electrodes. In addition, we will briefly outline the recent development on directly examining membrane-bound fractions of cyt P450s in association with CPR in the form of 'liver microsomes' (subcellular fractions of liver) and 'supersomes' (engineered bactosomes with a specific cyt P450 overexpressed with CPR) for chemical/drug toxicity screening and electrocatalytic applications.

2 Cyt P450 Catalytic Cycle

The catalytic cycle of cyt P450s (Scheme 1) involves substrate binding to the enzyme active site that is in close vicinity above the heme porphyrin ring. This is followed by a one electron reduction mediated by CPR from nicotinamide adenine



Scheme 1 Proposed cytochrome P450 catalytic cycle

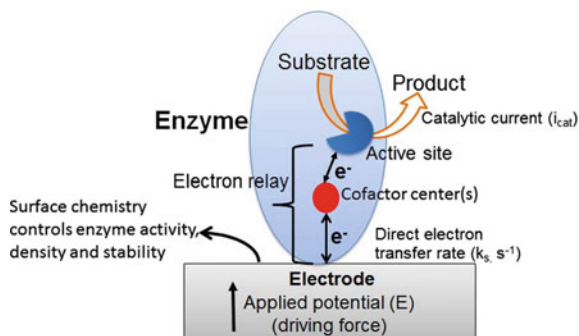
dinucleotide hydrogen phosphate (NADPH) to form the cyt P450-Fe^{II} heme form. Dioxygen binding to the reduced P450-Fe^{II} heme and a second electron reduction by CPR and protonation results in cyt P450-Fe^{III}-hydroperoxo complex. In some cases, cytochrome b₅ can act as the second electron donor. Further protonation followed by elimination of a water molecule has been shown to yield the reactive oxidant form, cyt P450-ferryloxy radical cation, ⁺⁺(P450-Fe^{IV}=O) (Scheme 1). This ferryloxy cyt P450 can readily oxygenate bound substrate RH to ROH. In contrast to membrane-bound human cyt P450s, the soluble bacterial cyt P450 called cyt P450_{cam} or CYP101 (here ‘cam’ stands for camphor binding cyt P450) utilizes the iron–sulfur protein putidaredoxin as a redox partner to mediate electrons from nicotinamide adenine dinucleotide hydrogen (NADH). Moreover, mammalian cyt P450_{scc}, sterol 27-hydroxylase and cyt P45011β are mitochondrial P450s that utilize a non-heme iron sulfur redox protein and not CPR [1, 10]. The peroxo form of cyt P450 is termed as ‘compound 0’ and the ferryloxy radical cation form is called ‘compound 1’ due to similarities with other heme-containing proteins [5, 11]. With purified cyt P450 enzymes, one can generate the ferryloxy form by simply using hydrogen peroxide as a reagent [12]. Investigation on the reactivity toward C–H bond activation, electronic structure, and physicochemical properties of compound 1 has been an intriguing area of research [13].

2.1 *Electrochemical Investigation of cyt P450 Enzymes*

Protein film electrochemistry (PFE) is an excellent method for studying electrochemical and catalytic properties of enzymes immobilized as films on electrodes [14–17]. PFE overcomes several disadvantages of studying proteins present in a solution. For example, the diffusion barrier for large protein molecules in solution to migrate to and from electrode is eliminated when the protein is attached to an electrode surface as a film. One can avoid electrode fouling from the denaturation of enzyme molecules on the electrode surface by controlling the surface properties of electrodes. In addition, PFE requires only a small amount of enzyme (a few μL of enzyme in the concentration range 0.5–3.0 mg mL^{−1} have been shown to be sufficient). Most importantly, the isolation of products from an electrocatalytic reaction is relatively straightforward in PFE as the enzyme component is not present in the same reaction solution as the reactant.

Accordingly, the stability and bioactive conformation of an immobilized enzyme needs to be retained on the electrode surface for catalytic conversion of a substrate into product(s). Hence the surface properties of electrode materials can directly influence the redox and catalytic activities of immobilized cyt P450 films. Figure 1 schematically illustrates the study of enzymes by PFE for direct electron transfer (ET) (between electrode and enzyme redox site) and subsequently facilitated electrocatalytic properties in the presence of a substrate.

Fig. 1 Schematic representation of studying enzyme electrochemistry and electrocatalysis



2.2 Development of PFE to Investigate Purified cyt P450 Films on Electrodes

Prior to the 1990s, the electrochemical investigations of enzymes present in solutions were shown to be limited by the denaturation of enzymes upon contact with electrode and by diffusion issues due to the large size of enzymes with the requirement for large sample volume [18, 19]. Later, the purity of enzyme and surface chemistry used for the design of electrodes have been shown to play crucial roles in retaining the biocatalytic properties of immobilized enzymes [20–22]. In cases where direct ET to cyt P450-heme center were not achievable, several enzyme and small molecule ET mediators were employed to mediate direct ET between the cyt P450-heme center and electrode, and thus facilitate catalytic reactions of cyt P450s [23–27]. The first direct ET kinetics of P450_{cam} in solution was achieved by Hill et al. who reported the voltammetry of dissolved, purified P450_{cam} in buffer at pH 6 °C [28]. The schematic representations of electrochemical setup for examining the direct cyt P450 electrochemistry in anaerobic buffer (N₂ or Ar atmosphere) and electrocatalytic properties in oxygen atmosphere and substrate by PFE with electrode rotation (to overcome substrate mass transport limitation) are shown in Fig. 2a and b, respectively.

For electrochemical studies of cyt P450 enzymes as films on electrodes, both covalent and non-covalent strategies (e.g., electrostatic, hydrophobic, and coated films) and composite films of cyt P450s mixed with other reagents (e.g., surfactants, polyions, nanomaterials) have been examined [29, 30]. Self-assembled monolayers covalently attached with cyt P450 2C9 on gold electrodes [31, 32] and those modified with maleimide compounds to achieve linking cyt P450s via cysteine residues have been shown [33–35]. So far only a tip of an iceberg is explored in cyt P450 electrocatalysis, and there remains numerous new and efficient surface chemistry strategies to be explored to achieve practically useful cyt P450 biosensors and catalytic reactors with long-term stability and scalability.

Our group reported the first direct electrochemistry of bacterial cyt P450_{cam} films mixed with vesicle dispersions of lipids [e.g., didodecyldimethylammonium bromide (DDAB)] on pyrolytic graphite (PG) electrodes [36]. We also showed the first

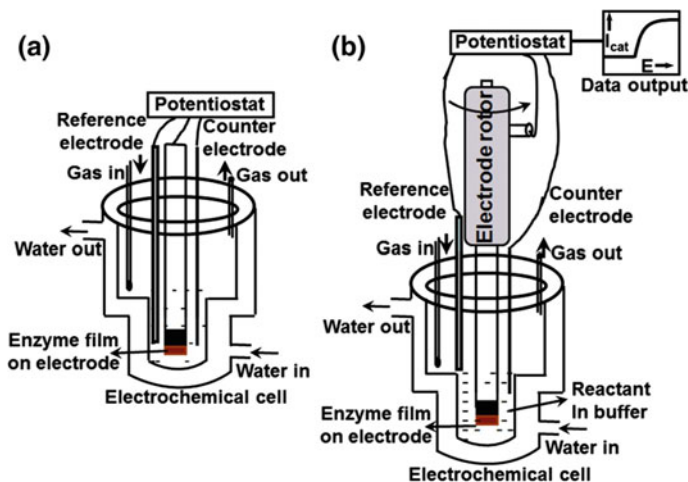


Fig. 2 Experimental setup for **a** studying direct electrochemistry of cyt P450 films on electrodes by cyclic voltammetry in N_2 or Ar atmosphere purged buffer solution and **b** rotating disk voltammetry to examine electrocatalysis of cyt P450 films on electrodes under steady-state conditions achieved by rotating the electrodes

direct voltammetry of cyt P450_{cam} assembled electrostatically as layer-by-layer (LbL) films with polyions on basal plane PG electrodes [37]. Following this, the electrocatalysis by LbL films of bacterial and human cyt P450s with polyions were demonstrated [38–40]. Prior representative reviews by us and others discussed the direct electrochemistry, biosensing, and electrocatalysis of cyt P450 enzymes and engineered supersomes and cyt P450 covalently linked with CPR as a fusion protein system [41–46]. Therefore, in this chapter, we aim to provide an outlook of different ligand binding and catalytic pathways that are driven electrochemically using purified human P450 enzymes and those present in membrane fractions with CPR.

2.3 Characterization of Ultrathin LbL Films of Human cyt P450 Enzymes with Negatively Charged Poly(styrene sulfonate) Polyions

Since characterizing the formation and identifying the optimal film construction conditions for cyt P450 film assembly with polyions on a graphite electrode surface is tedious, the application of quartz crystal microbalance (QCM) with gold disk-impregnated quartz crystals has been an accepted procedure. Although the gold surface of QCM does not account for the surface roughness of graphite, chemical functional groups, and defects on graphite electrodes, the QCM characterization allows the identification of optimum conditions such as concentrations of

Table 1 Average characteristics of enzyme LbL assemblies from QCM studies (Reprinted with permission from the American Chemical Society, Ref. [47], Copyright 2009)

Film architecture	Nominal film thickness (nm)	Amount of enzyme (nmol cm ⁻²)	Enzyme conc. in film (μmol cm ⁻³)
PEI/(PSS/1A2) ₄	24 ± 1	0.11 ± 0.01	46 ± 4
PEI/(PSS/2E1) ₄	24 ± 3	0.12 ± 0.02	51 ± 8
PSS/(PEI/cam) ₄	9 ± 1	0.05 ± 0.003	55 ± 4

polyions and enzymes, pH and ionic strength of buffer solutions and enzymes, adsorption time, and adsorption temperature to attain stable and reproducible LbL films of cyt P450 enzymes with polyions. Moreover, the nominal film thickness of each layer, and amounts of enzymes and polyions in the assembly can be estimated by QCM measurements [47]. These optimized conditions can then be used on graphite electrodes to construct reproducible assemblies of cyt 450s with polyions for electrochemical investigation.

As an example, Table 1 is presented with the nominal film thickness and enzyme concentration of four bilayers of positively charged human cyt P450 1A2 or cyt P450 2E1 (at pH 7.0) assembled LbL with negative polystyrene sulfonate (PSS) on a polycation (polyethylene imine, PEI) adsorbed layer on gold surface of quartz crystals. Also shown is the LbL film of negatively charged bacterial cyt P450_{cam} (at pH 7.0) assembled with PEI on PSS adsorbed gold surface of quartz crystals. The cyt P450_{cam} film assembly was found to be thinner than the film assembly of human cyt P450s with polyions that suggested the influence of net protein charge and conformation toward film thickness.

2.4 *Electrocatalytic Pathways in Purified cyt P450 Films on Electrodes*

2.4.1 Direct Electron Transfer

Under anaerobic conditions, when the heme center of cyt P450 is within the ET proximity from electrode surface, one can observe electron injection to cyt P450-ferric heme form at a potential around -0.3 to -0.35 V at pH 7.0 (reduction wave) versus standard calomel electrode (SCE) (a useful note: $E_{\text{SHE}} = E_{\text{Ag/AgCl}}(\text{saturated KCl}) + 206$ mV and $E_{\text{SHE}} = E_{\text{SCE(saturated KCl)}} + 241$ mV at 25 °C [48]). The electronic communication from the electrode to cyt P450-heme center can involve tunneling (through bond) or hopping (through space) mechanism depending on the mode of attachment and environment of cyt P450 on the electrode surface. Reversing the reduction scan direction can allow us to monitor the oxidation of the reduced cyt P450-ferrous form back to cyt P450-ferric state (oxidation wave, electrons are now given back to the electrode) at a more positive potential with respect to the reduction wave. Such a reversible redox property that does not require

any ET mediator to shuttle electrons between electrode and cyt P450-heme cofactor is called direct ET process. The technique that facilitates the study of reversible redox properties of any electroactive molecule is called cyclic voltammetry.

The formal or midpoint potential (E°) of a redox species is calculated by averaging the reduction and oxidative peak potentials. The rate at which an ET occurs between electrode and cyt P450-heme center can be determined by acquiring the cyclic voltammograms with increasing scan rates and by applying the Butler–Volmer and Marcus theories. One can also obtain information about non-electrochemical processes associated with an electrochemical event from cyclic voltammetry. One example is proton-coupled ET.

Figure 3a represents the anaerobic cyclic voltammograms (CVs) with increasing scan rates for human cyt P450 2E1 electrostatically assembled as LbL films with a negative polyanion (PSS) on freshly polished basal plane pyrolytic graphite electrodes. Here the voltammograms are background subtracted to eliminate the coexisting non-faradic charging currents as illustrated in Fig. 3c. Without the cyt P450 2E1 film, i.e., the polyethylene imine and poly(styrene sulfonate) bilayer coated electrodes alone do not show any peaks in the voltammograms (Fig. 3c).

The E° of cyt P450 2E1 in these films was found to be -0.35 V versus SCE. From the increase in peak separation with scan rates, the direct ET rate constant was calculated to be 18 s^{-1} . From the pH-dependent shifts in formal potentials, we confirmed the proton-coupled ET process of these cyt P450 2E1 films as shown in Fig. 3b. For a Nernstian process with equal number of protons and electrons, the shift in E° per pH is calculated to be 59 mV [48] and the designed cyt P450 2E1 films showed a shift of 50 mV pH^{-1} , which is slightly less than the ideal value of 59 mV [47].

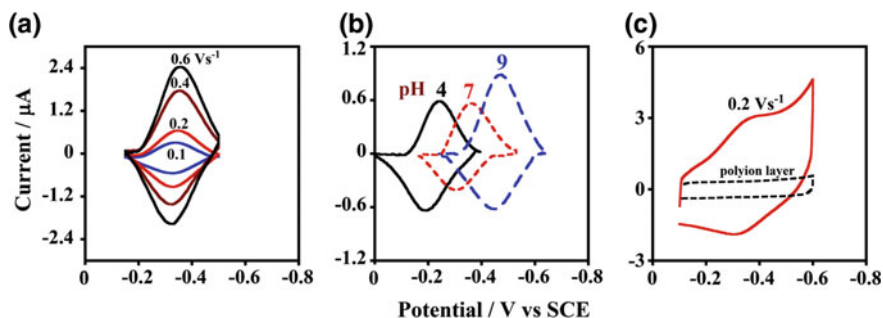


Fig. 3 **a** Background subtracted surface-confined CVs of cyt P450 2E1 assembled with polyions on pyrolytic graphite electrodes in anaerobic 50 mM potassium phosphate buffer, 0.1 M NaCl, pH 7.0. **b** Corresponding cyclic voltammograms at different pH values showing the proton coupled electron transfer in the cyt P450 2E1 films. **c** Cyclic voltammograms of cyt P450 2E1 film shown with coexisting non-faradic or charging current at 0.2 V s^{-1} scan rate and electrodes coated with a bilayer of polyions showing no redox peaks in the absence of cyt P450 2E1. Reprinted with permission from the American Chemical Society, Ref. [47], Copyright 2009

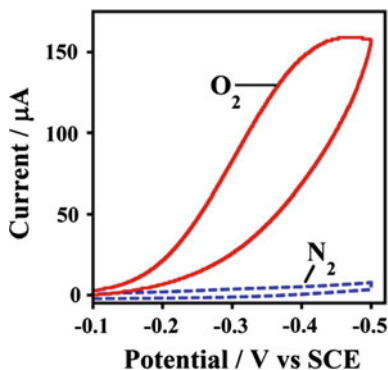
2.4.2 Electrochemical Monitoring of Ligand Binding to Human cyt P450s

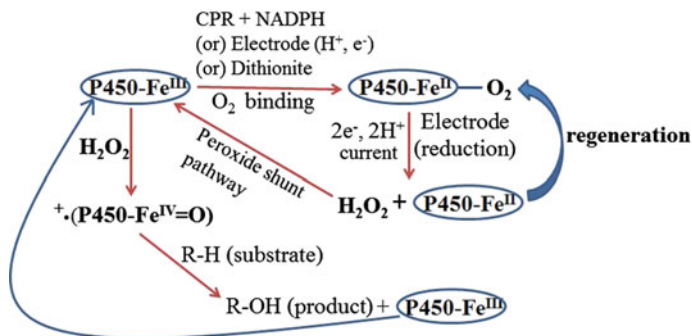
O₂ and peroxides Oxygen acts as a crucial ligand in cyt P450 catalysis by enabling the formation of reactive $^{++}(\text{cyt P450-Fe}^{\text{IV}}=\text{O})$ oxidant form (Fig. 1) involving a total of 2-electron reduction of cyt P450-ferric state. This reduction under in vivo conditions has been shown to be mediated by CPR using NADPH as the electron donor [3]. For spectrochemical studies, the reduction of cyt P450 in solution can be carried by chemical reducing agents (e.g., sodium dithionite is commonly used). Electrochemically, the reduction of cyt P450 is achieved by application of potential to the electrode coated with cyt P450 films.

The electrochemical binding of O₂ to reduced cyt P450 results in the formation of cyt P450-Fe^{II}-O₂ complex. This complex was shown to rapidly undergo further reduction on the electrode at the cyt P450 reduction potential to form hydrogen peroxide along with the regeneration of reduced cyt P450-Fe^{II} to bind new O₂ molecules [47]. The resulting high current (much greater than direct ET currents shown in Fig. 4), called catalytic reduction current, is proportional to the available oxygen. The catalytic currents are monitored by cyclic voltammetry as an increase in reduction peak current in the presence of oxygen with the disappearance of the oxidation peak, this is because the regenerated cyt P450-Fe^{II} rapidly binds new oxygen molecules and not available to undergo oxidation in the reverse scan.

Figure 4 shows the electrocatalytic oxygen reduction by cyt P450 2E1 films assembled LbL with polyions. We can understand that the current is much larger than the direct ET currents observed for the same film in anaerobic nitrogen atmosphere. Thus, it is difficult to obtain high direct ET currents in anaerobic CVs of cyt P450 protein films due to the presence of significant non-faradic or charging currents, which can be overcome by exploiting large electrocatalytic currents from the high enzyme turnover rate as shown in Scheme 2. Due to this reason, electrochemical biosensors are designed based on electrocatalytic currents rather than direct ET currents to offer high sensitivity. Scheme 2 proposes the catalytic oxygen binding and reduction by cyt P450 enzymes, and the associated peroxide formation and its role in the cyt P450-catalyzed conversion of substrate to products.

Fig. 4 CVs of cyt P450 2E1 assembled with polyions on pyrolytic graphite electrodes in nitrogen atmosphere and in saturated oxygen, 50 mM potassium phosphate buffer, 0.1 M NaCl, pH 7.0, scan rate 0.1 V s⁻¹. Reprinted with permission from the American Chemical Society, Ref. [47], Copyright 2009





Scheme 2 Pathways for biocatalytic oxygen binding and reduction and subsequently formed peroxide in the cyt P450 activation to catalyze substrate conversion

To overcome the mass transport limitation of ligands (e.g., O_2 , H_2O_2) or substrates from solution to reach cyt P450 molecules present on an electrode surface, the electrode is rotated at certain speeds (usually in the range 1000–3000 rpm) in electrocatalytic reactions to obtain steady-state currents. Stirring the electrolyte solution has also been shown to facilitate mass transport by convection. The rotation rate-dependent catalytic currents is governed by the Levich equation, which relates the rates of interfacial electron exchange, enzyme kinetics, and substrate mass transport to steady-state catalytic currents [48–50].

Similar to oxygen, the direct peroxide reduction kinetics by cyt P450 films can be examined electrochemically. Due to many radical intermediates formation in the case of hydrogen peroxide, such reduction kinetics can be preferably studied using *t*-butyl hydroperoxide (tBuOOH) which mainly forms *t*-butanol (t-BuOH) as the cyt P450 reduction product. Figure 5 shows the catalytic reduction currents with

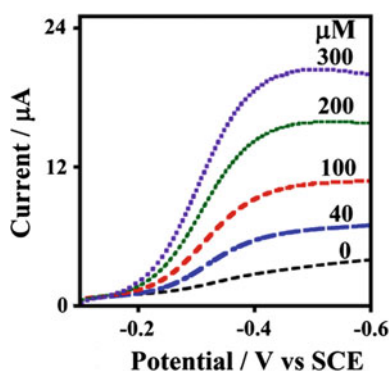
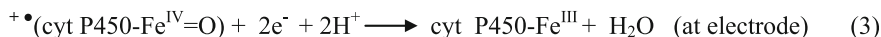
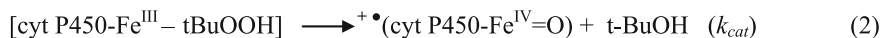


Fig. 5 Representative electrocatalytic voltammograms of cyt P450 2E1 films assembled with polyions on pyrolytic graphite electrodes for *t*-butyl hydroperoxide reduction at 1000 rpm in anaerobic 50 mM potassium phosphate buffer, 0.1 M NaCl, pH 7.0 at 25 °C. Reprinted with permission from the American Chemical Society, Ref. [47], copyright 2009



Scheme 3 Peroxide binding and reduction by cyt P450 enzymes

increasing t-butyl hydroperoxide concentrations by cyt P450 2E1 films on electrodes rotated at 1000 rpm. The cyt P450 oxidation in the presence of organic peroxide and the associated kinetic parameters are shown in Scheme 3.

In the Scheme 3, Eq. 1 denotes the binding of t-BuOOH to ferric cyt P450 enzyme to form the cyt P450-substrate complex characterized by the Michaelis–Menten affinity constant, K_M . The conversion of t-BuOOH into t-BuOH is characterized by k_{cat} with the formation of ferrylcytochrome P450 radical cation (Eq. 2). This oxo species is subsequently reduced by the electrode yielding catalytic peroxide reduction currents with the regeneration of cyt P450-ferric form (Eq. 3).

Carbon monoxide The name of cyt P450 originates from the characteristic Soret absorbance band at 450 nm of reduced high spin (HS) pentacoordinate ferrous form (cyt P450-Fe^{II}) upon binding to CO forming a low spin (LS) hexacoordinate ferrous-CO form [51]. The formation of cyt P450 Fe^{II}-CO complex at 450 nm is experimentally measured as a difference absorbance measured against the reduced form of the cyt P450-ferrous form as the reference. Figure 6a shows the UV-vis absorbance spectrum of cyt P450 1A2-Fe^{III} heme form in a polyion LbL film constructed on transparent silica slides similar to the procedure followed on graphite electrodes.

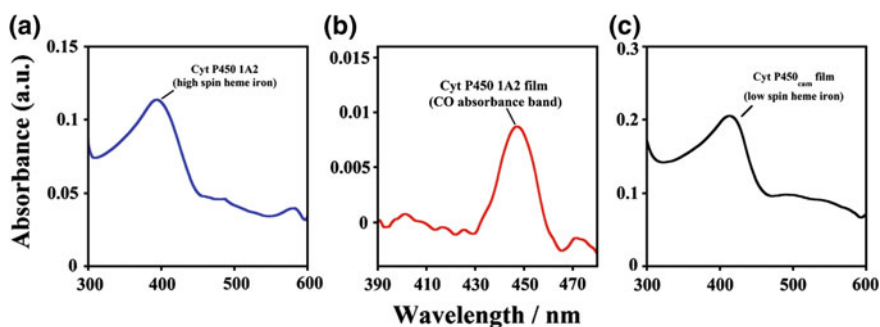


Fig. 6 UV-vis spectra of LbL films of cyt P450 enzymes on aminosilane-functionalized fused silica slides: **a** high spin ferric form of purified human cyt P450 1A2 assembled with polyions; **b** CO difference spectrum of human cyt P450 1A2 assembled with polyions after reducing to the ferrous form by sodium dithionite and purging pH 7.0 buffer with CO. **c** Low spin ferric form of purified bacterial cyt P450_{cam} assembled with polyions. Reprinted with permission from the American Chemical Society, Ref. [47], Copyright 2009

The absorbance maximum at 394 corresponds to the native HS heme iron in cyt P450 1A2 [6, 7, 52]. Figure 6c shows the LS absorbance spectrum ($\lambda_{\text{max}} \sim 418$ nm) of purified bacterial cyt P450_{cam} assembled with polyions on silica slides. Figure 6b shows the corresponding difference absorbance band at 450 nm in CO atmosphere of the sodium dithionite-reduced cyt P450 1A2/polyion LbL film. In the cases of denatured cyt P450s, the complex with CO displays a band around 420 nm. During the recombinant human cyt P450 purification, the CO absorbance band is used to assess the level of cyt P450 expression in bacterial membrane usually by using CPR and NADPH reconstitution system to reduce cyt P450 and allow CO binding with the heme cofactor.

Electrochemically, the reduction of cyt P450s by applied negative potential in the presence of CO forms cyt P450-Fe^{II}-CO complex which can be identified from the positive shift in formal potential by about 50 mV with respect to the formal potential obtained under anaerobic conditions (nitrogen or argon). Unlike the positive potential shift observed for CO binding to reduced cyt P450-ferrous heme, substrate binding to the active site of cyt P450 has been suggested to cause potential shifts only if the spin state of heme iron is altered [28, 53]. Figure 7 shows the CVs of cyt P450_{cam} in a surfactant film in nitrogen and in the presence of CO from which one can understand the formal potential shift caused by CO complex with cyt P450. Similar potential shifts were observed for LbL films of purified human cyt P450 with polyions on electrodes [47].

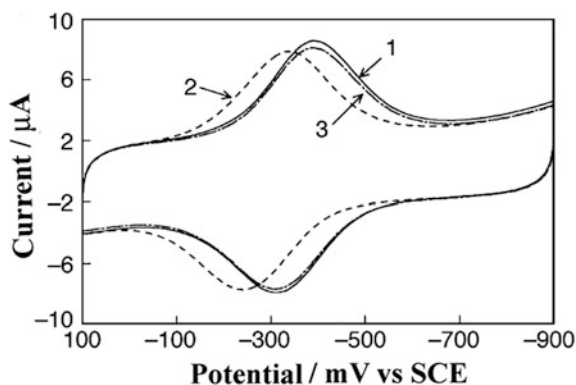


Fig. 7 CVs of basal plane pyrolytic graphite electrodes at 100 mV s^{-1} in pH 7 buffer, 0.1 M KCl. 1 substrate-free cyt P450_{cam} in oxygen-free buffer containing no enzyme; 2 cyt P450_{cam}-surfactant mixed film on same electrode after solution was purged with CO for 5 min; 3 same electrode after solution was purged with N₂ for 20 min to remove CO. Adapted from Ref. [36], Royal Society of Chemistry Publishers, Copyright 1997

2.5 *Cyt P450 Heme Iron Spin State: Spectral and Electrochemical Properties*

The spectroscopic and redox properties of cyt P450 enzymes is strongly influenced by the heme iron spin state [54–56]. The spin state also infers about the axial coordination of ligands to the heme iron cofactor. The LS state of cyt P450 heme represents a hexacoordinated iron species. Coordination of water as the axial ligand can stabilize the LS state of heme cofactor. Removal of the water ligand results in the HS pentacoordinated geometry. Similarly, coordination of CO to reduced pentacoordinate HS cyt P450 ferrous iron forms the hexacoordinate LS cyt P450 ferrous-CO complex. This spin state change and cyt P450 Fe^{II}-CO complex formation can be observed spectroscopically as described in the preceding section and is significant enough to also positively shift the redox potential of cyt P450 enzymes.

The catalytic cycle and spin state mechanisms were originally derived based on the well-studied bacterial cyt P450_{cam} which exhibits predominant LS heme iron in the substrate-free state [56]. In contrast, recombinantly expressed human cyt P450 1A2 has been shown to exhibit predominantly HS heme iron and human cyt P450 2E1 in a mixed spin isoform [9, 52]. Also, it is noteworthy to mention that the bacterial cyt P450_{cam} has been well characterized prior to human cyt P450 enzymes. This is because of the ease of isolation, expression, and purification of cyt P450_{cam} in large quantities, and the successful establishment of high-resolution crystal structures and catalytic properties of this enzyme well before the human cyt P450s.

With regard to the effect of substrate binding in altering the spin state of cyt P450 enzymes, there is even more interesting findings reported in the literature. In this, the soluble bacterial cyt P450_{cam} has been shown to undergo change in spin states and redox potentials upon substrate binding. In contrast, the binding of substrates to membrane-bound human cyt P450 enzymes rarely showed shifts in redox potentials [54–56]. The absence of redox potential shift with substrate binding could be due to differences in the resting spin states of native membrane-bound cyt P450s and suggests that the spin state conversion is not significant to change redox potentials of heme iron cofactor.

Johnson et al. pointed out the need to consider the influences of experimental conditions and methodologies used in monitoring the redox potential shifts of cyt P450 enzymes upon substrate binding [56]. They also discussed that in the case of bacterial cyt P450_{cam}, a redox potential shift of 130 mV was noted upon camphor binding to cyt P450_{cam} present in solution [54, 55], while it was only 23 mV on a hydrophobic methyltriethoxysilane electrode [57], and no shift on a clay-modified electrode [58]. Regardless of the presence of redox potential shifts upon substrate binding, many cyt P450 coated electrodes showed catalytic activity, which suggests that the absence of redox potential shifts in cyt P450 enzymes upon substrate binding does not necessarily mean that the substrate is not bound or the catalytic activity is absent [59].

Using cyclic voltammetric examination of LbL films of bacterial cyt P450_{cam}, human cyt P450 1A2, and cyt P450 2E1 with increasing scan rates under anaerobic nitrogen atmosphere, we recently showed that the native heme iron spin state differences among these three cyt P450s could affect the direct electrochemical reduction rates [47]. We observed that the LS state of bacterial cyt P450_{cam} offered 40 times faster reduction rates than the HS cyt P450 1A2 with the mixed spin cyt P450 2E1 exhibiting an intermediate reduction rate. We suggested the contribution of smaller activation energy barrier required to efficiently reduce LS cyt P450-heme center than the HS cyt P450-heme [60], the influences of the rates of electrochemical and chemical conformational equilibria explained by a square scheme, and possible protein structural differences and orientations on electrodes.

2.6 *Electrode-Driven Substrate to Product Conversion by Human cyt P450 Films*

To convert a substrate into product by cyt P450 films immobilized on electrodes, the application of potential slightly more negative than the formal potential (usually by about 100–200 mV to overcome any overpotential barrier) of cyt P450 with a constant supply of oxygen are required. One can also activate the catalytic pathway of purified cyt P450 films by directly supplying hydrogen peroxide along with substrate [61, 62].

Seminal studies using films of bilayer membranes mixed with cyt P450_{cam} on electrodes or LbL films of cyt P450_{cam} with polyions showed the electrocatalytic reduction of peroxides, oxygen, and trichloroacetic acid [36, 37]. Also, the electrochemical conversion of styrene to styrene oxide by cyt P450_{cam} LbL films was demonstrated. Following this, the epoxidation of styrene mediated by initial catalytic reduction of dioxygen to H₂O₂ by human cyt P450 1A2 films assembled LbL with PSS on carbon cloth electrodes (0.7 × 6.0 cm²) was shown [38–40]. Here, the carbon cloth electrode offers large surface area to adsorb high quantity of cyt P450 to produce sufficient reaction products that are detectable by common chromatographic methods.

In addition to obtaining products from electrochemical cyt P450-catalyzed reactions, it has been shown that one can observe current signal increase with substrate (e.g., drug) concentration. The caveat here is to clearly differentiate the enzyme turnover currents toward a substrate by subtracting the coexisting large background oxygen reduction currents. Thus, electrochemical biosensing of drug metabolism and inhibition can be achieved using films of cyt P450 on electrodes. We demonstrated the first electrochemical biosensor made of human cyt P450 3A4 films on gold electrodes that provided the verapamil drug concentration-dependent increases in currents measured by cyclic voltammetry (Fig. 8a) and chronoamperometry (Fig. 8b and c) [59]. This verapamil cyt P450 biosensor was validated by identifying the verapamil dealkylation product, norverapamil.

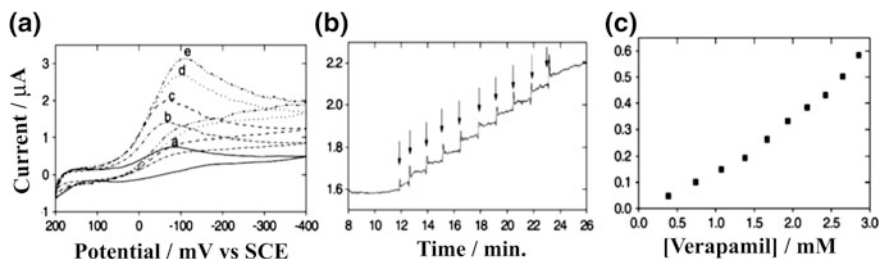


Fig. 8 **a** Voltammetric response of a cyt P450 3A4 biosensor upon addition of verapamil in 50 mM phosphate buffer, 0.1 M KCl, pH 7.4. *a* in the absence of oxygen and substrate, following injection of *b* 10 mL of oxygen gas (0 control), *c* 0.87, *d* 2.48, and *e* 3.21 mM verapamil. **b** Steady-state amperometric responses (current versus time plot at constant applied potential, -405 mV versus SCE) of the cyt P450 3A4 biosensor upon addition of verapamil, a cyt P450 3A4 substrate. **c** Calibration curve for verapamil obtained from the data shown in **b**. Reprinted with permission from Ref. [59], Elsevier Publishers, Copyright 2003

Later, Gilardi et al. reported cyt P450 2E1-catalyzed electrocatalytic conversion of p-nitrophenol to p-nitrocatechol with product identification and also showed increase in currents with increasing concentration of p-nitrophenol [34]. For this study, the authors designed cyt P450 2E1 films covalently attached to gold surface modified with cystamine and end maleimide groups. Paternolli et al. developed an electrochemical biosensor made of Langmuir–Blodgett (LB) films of cyt P450_{SCC} to detect cholesterol [63]. Similarly, amperometric current increase for cyt P450 2B6 bound to gold nanoparticle–chitosan films on the surface of glassy carbon electrodes with various concentrations of drugs, bupropion, lidocaine, and cyclophosphamide, has been reported [64].

Drop-coated films of human cyt P450 3A4 in an epoxy polymer-acetylene black composite matrix were shown to exhibit direct ET and detect diethylstilbestrol substrate [65]. Similarly, glassy carbon electrodes containing drop-coated films of human cyt P450 2C9 mixed with polyacrylamide and ammonium persulfate providing a hydrogel environment was shown to be useful for detection of bisphenol A [66]. In addition to direct electrochemical and sensing properties, the authors have shown spectral data confirming the near native conformation of cyt P450 2C9 mixed in the hydrogel films. Such electrochemical biosensors are quite useful for applications such as drug development and environmental pollutant screening as cyt P450 enzymes are not only drug metabolizing enzymes but also are involved in the lipophilic pollutant clearance in humans [67–70].

2.7 Microsomal Electrochemistry and Electrocatalysis

Electrochemical studies have shown that the catalytic efficiency is significantly enhanced when electrons are mediated to cyt P450 enzymes via cytochrome P450-reductase [71] or cyt P450 fused with CPR domain [72] as against the direct

reduction of cyt P450 by electrodes. This was proposed to be due to longer lived cyt P450-peroxo species (Fig. 1) [72]. Thus, the direct application of membrane-bound subcellular fractions containing cyt P450 and CPR on electrodes may allow a cost-effective, straightforward design of biosensors and in the identification of the roles of several of cyt P450 isoforms on drug metabolism and inhibition [73]. For large-scale applications, the use of engineered supersomes containing a specific, overexpressed cyt P450 along with CPR in membranes may be advantageous to produce large quantities of cyt P450 with reductase system.

We showed that engineered microsomes expressed with human cyt P450 (1A2 or 3A4) plus CPR (the so-called ‘supersomes’) assembled LbL with polyions on electrodes can be used to catalyze epoxidation of styrene to styrene oxide [74]. However, such supersomal films on electrodes displayed a formal potential of -0.49 V versus SCE, which was more negative than the purified cyt P450 films on similar electrodes. Moreover, the redox peaks of supersomal films did not exhibit catalytic O_2 reduction or peroxide reduction currents and the formal potential did not shift in the presence of CO. These are not in favor of the characteristics heme cofactor properties of cyt P450 present in the supersomes. Nevertheless, these supersomal films catalyzed the electrochemical epoxidation of styrene to styrene oxide in the presence of oxygen, typical of cyt P450 activity (1A2 or 3A4).

Following the supersomes study, we explored more complex pooled rat liver microsomes (RLM) containing various cyt P450s, other monooxygenases, CPR, and cyt b_5 . Again, we found that the electrochemical and electrocatalytic properties of RLM were similar to those of supersomes displaying reductase-like electrochemistry and not cyt P450. Later, Mie et al. showed that supersomes containing cyt P450 3A4 and CPR (similar system to our 2005 report), adsorbed on hydrophobic surfaces representing aromatic thiolate groups on gold electrodes, exhibited both the CPR-like electrochemistry and cyt P450 properties with the positive potential shift in the presence of CO [75]. The authors demonstrated the formation of 6 β -hydroxytestosterone from the electrocatalysis of testosterone by the supersomal films on electrodes.

Another approach was based on fusion protein systems by which cyt P450 has been linked to the reductase domain of bacterial CYP102A1 or with flavodoxin to achieve efficient direct electron transport between the cyt P450 heme center and electrode via the reductase domain, and conversion of erythromycin to formaldehyde by N-demethylation [72]. The engineering of reductase fusion domain with cyt P450 was suggested to offer improved catalytic efficiency by controlling the lifetime of the iron-oxo complex of cyt P450 compared to the electrocatalysis by cyt P450 alone.

Therefore, with the goal to identify and delineate cyt P450 electrochemistry coexisting with microsomal CPR in a microsomal film, we electrostatically assembled LbL films of purified cyt P450 2E1 or 1A2 and microsomal CPR on pyrolytic graphite electrodes modified with an initial polymer bilayer surface to avoid direct contact of cyt P450 with electrode, which could unfold the enzyme and expose heme [71]. Figure 9 shows the schematic of the designed LbL films of cyt P450 and CPR. Here the surface polyanion bilayer also facilitated the initial

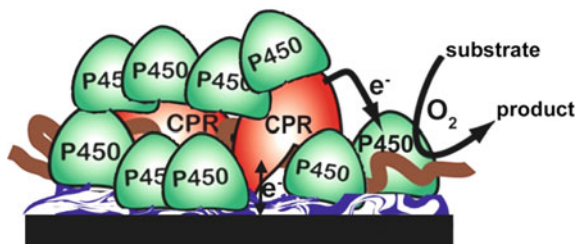


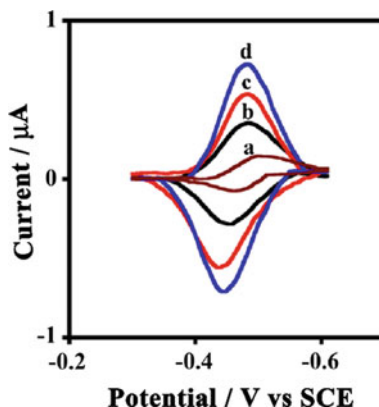
Fig. 9 Schematic representation of LbL films of cyt P450 and CPR on pyrolytic graphite electrodes. Films are assembled electrostatically from CPR microsomes and pure cyt P450s on polyanion bilayer surface of pyrolytic graphite disk electrodes

electrostatic adsorption of positively charged human cyt P450 1A2 or 2E1 at pH 7.0 (since $pI > 7.0$).

Figure 10 represents the background subtracted CVs of the LbL films of cyt P450 with CPR. While, the cyt P450 and CPR redox peaks are not separable in the voltammograms, we were able to provide the first unambiguous mechanistic information in understanding the microsomal CPR-mediated biocatalytic pathway of cyt P450 mimicked on the designed electrodes. For this, we systematically examined the films of microsomal CPR alone, purified cyt P450 1A2 or 2E1 alone, and the cyt P450s assembled with CPR under similar conditions on electrodes. Based on formal potentials, direct ET rates, ligand binding properties, substrate conversion and turnover rates, simulation of experimental voltammograms, and by spectroscopic studies, we provided evidences for the mimicking of *in vivo* cyt P450 catalytic pathway on the designed LbL film electrodes as briefly discussed below [71].

The formal potentials of the LbL films of cyt P450 (1A2 or 2E1) with CPR was in the range -0.47 to -0.49 V versus SCE (Fig. 10). This is the same as the formal potentials of only microsomal CPR film with or without cyt b_5 present in it. Moreover, the direct ET rates of LbL films of only microsomal CPR or cyt P450

Fig. 10 Background subtracted CVs in anaerobic pH 7.0 buffer +0.1 M NaCl for LbL films of *a* polyions and only microsomal CPR with no cyt P450 (at 0.3 Vs^{-1} scan rate), and *b-d* LbL films of cyt P450 1A2 assembled with microsomal CPR at scan rates *b* 0.1, *c* 0.2, and *d* 0.3 Vs^{-1} . Reprinted with permission from the American Chemical Society, Ref. [71], Copyright 2011



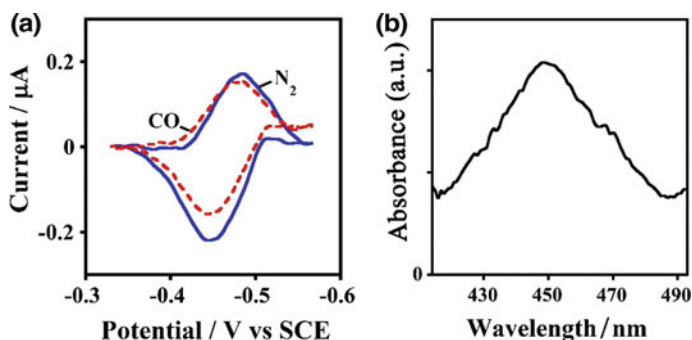
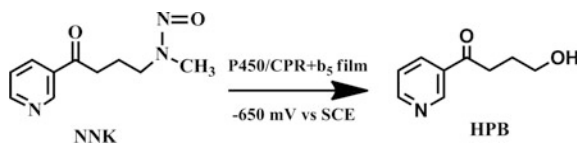


Fig. 11 **a** Background subtracted CVs in pH 7.0 buffer +0.1 M NaCl for LbL films of cyt P450 1A2 and microsomal CPR assembled on electrodes in the presence of nitrogen and CO. **b** Corresponding CO difference spectra of the LbL films assembled on aminosilane-fused silica slides (analogous to the assembly on electrodes) in the presence of NADPH. Reprinted with permission from the American Chemical Society, Ref. [71], Copyright 2011

assembled with CPR were nearly the same and $\sim 40 \text{ s}^{-1}$. Upon CO purging to the LbL films of cyt P450s and microsomal CPR, no shift in the formal potential from anaerobic nitrogen voltammograms was observed (Fig. 11a). In contrast, such LbL films of cyt P450 with microsomal CPR assembled on silica slides displayed the characteristic cyt P450 difference absorbance band at around 450 nm in the presence of CO and NADPH (Fig. 11b). This indicated that CPR in the LbL film with cyt P450 received electrons from NADPH and reduced cyt P450 to facilitate the binding of CO. The spectral and electrochemical properties inferred that the communication of microsomal CPR with the electrode was kinetically favored over the cyt P450 in the assembled films.

More interestingly, at an applied potential of -0.65 V versus SCE in the presence of oxygen, the LbL films of pure cyt P450 2E1 and microsomal CPR were able to oxidize the cyt P450 2E1 substrate, 4-(methylnitrosamino)-1-(3-pyridyl)-1-butanone (NNK), into 4-hydroxy-1-(3-pyridyl)-1-butanone (HPB) as shown in Scheme 4. The product formation after the electrolysis was confirmed by capillary liquid chromatography (LC) coupled with mass spectrometry (Fig. 12, only LC data is shown). This reaction product would be only possible if electrons were transferred from the electrode-reduced CPR to cyt P450 2E1 to allow oxygen binding to the reduced cyt P450 2E1 and thus catalyze the conversion of NNK to HPB



Scheme 4 Electrode-driven cyt P450 catalytic cycle involving electron supply by electrode to CPR and then to cyt P450 in the presence of oxygen and NNK substrate

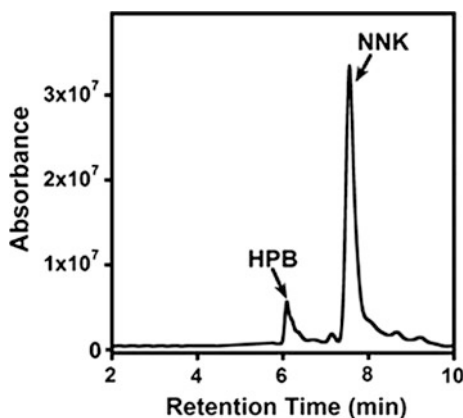


Fig. 12 Identification of 4-hydroxy-1-(3-pyridyl)-1-butanone (HPB): capillary LC-UV chromatogram (210–300 nm) of reaction mixture after 1 h. Electrolysis (−650 mV vs. SCE at 4 °C) of LbL films of cyt P450 2E1 and microsomal CPR on carbon cloth (2 cm²) in 2 mM NNK in O₂ purged pH 7.0 + 0.1 M NaCl buffer. Reprinted with permission from the American Chemical Society, Ref. [71], Copyright 2011

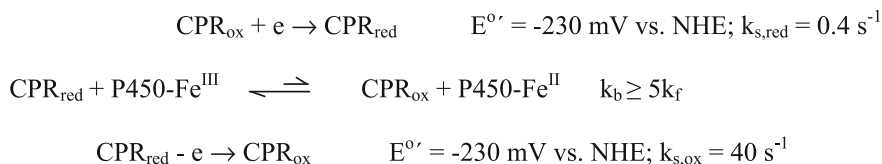
Table 2 Relative turnover rates for electrolysis and NADPH driven NNK oxidation in oxygen saturated 50 mM phosphate buffer plus 0.1 M NaCl, pH 7.0 for LbL films of cyt P450 2E1 with microsomal CPR (denoted as 2E1/CPR film)

Product	Electrolysis (−0.65 V vs. SCE)			NADPH assay
	2E1/CPR film	Polyion/CPR film	Polyion/2E1 film	2E1/CPR film
HPB found (nmol)	0.24 ± 0.04	0.003 ± 0.001	0.03 ± 0.01	0.14 ± 0.03
Turnover rate h ^{−1} (mol HPB) ^{−1} (mol P450) ^{−1}	57 ± 9	~0.7	7 ± 2.5	34 ± 6
H ₂ O ₂ found (mM)	0.75 ± 0.12	0.73 ± 0.10	0.30 ± 0.06	–

Reprinted with permission from the American Chemical Society, Ref. [71], Copyright 2011

metabolite. Moreover, the levels of hydrogen peroxide formed from the electrochemical reduction of O₂ in the electrolysis of NNK reaction solution was similar among electrodes featuring only polyion films with no protein present, only microsomal CPR and polyion LbL films with no cyt P450, and LbL films of cyt P450 2E1 with microsomal CPR (Table 2).

This observation confirmed that peroxide shunt pathway was not utilized in the NNK catalysis by LbL films of cyt P450 2E1 with microsomal CPR (Scheme 1) which would have otherwise caused less peroxide level to remain in the electrolyte solution compared to that produced with just polyion or microsomal CPR electrodes. Therefore, the electrochemically driven biocatalysis should have followed the natural CPR-mediated cyt P450 catalytic pathway in the designed electrostatically



Scheme 5 E_{rCEo} Simulation model for CVs of cyt P450/CPR films with best fit parameters [71]

assembled films of pure cyt P450 and microsomal CPR. Based on these results, we derived an electrochemical kinetic mechanism, E_{rCEo} , obtained by digital simulations of voltammograms that agreed well with the experimental CVs (Scheme 5) and provided additional insights that could not be understood from the experimental voltammetry alone (see Ref. [71] for more details).

It is important to note that the metabolites formed from the electrochemically-driven human cyt P450 catalytic products [either in the purified form or in microsomes with CPR] are the same as that observed in biochemical assays involving the incubation of microsomes with CPR, NADPH, and substrate [71, 75, 76]. This validates the unique advantage and simplicity of designing cyt P450 film electrodes for green synthesis of fine chemicals and specific biosensing applications. One other important advantage of the electrode-driven cyt P450 catalysis is in the offering of catalytic turnover rates that were comparable to or better than the hydrogen peroxide activation pathway with purified cyt P450 and solution assays utilizing NADPH and CPR [38–40, 43, 71, 77].

3 Summary

Protein film electrochemistry combined with appropriate electrode surface modifications to assemble purified cyt P450 enzymes and membranes containing cyt P450 and cyt P450-reductase have contributed to understanding of biocatalytic pathways of this important class of enzymes. Moreover, the differences in electrochemical and spectral properties of bacterial cyt P450_{cam} and human cyt P450 enzymes have been understood by combining voltammetry with spectroscopy techniques. Still evolving findings made by the scientific community so far have shed light in the fundamental understanding of electron transport in the major class of drug metabolizing cyt P450 enzymes, ligand and substrate binding characteristics, and broad electrocatalytic properties. Such understanding has potential applications in areas such as green stereoselective synthesis of fine and specialty chemicals, in the development of drug and pollutant biosensors, in bioremediation processes to remove toxic pollutants, and in the synthetic design of cyt P450-inspired biomimetic catalysts [78–80] and engineered cyt P450 systems for selective catalytic applications.

Acknowledgments The authors thank colleagues named in joint publications who collaborated on research in this area, and without whom progress would not have been possible. JFR thanks the National Institute of Environmental Health Sciences (NIEHS), NIH, USA, Grant No. ES03154 for financial support. SK is grateful for financial support by the National Institute of Diabetes and Digestive and Kidney Diseases of the National Institutes of Health under Award Number R15DK103386.

References

1. Ortiz de Montellano PR, De Voss JJ (2005) In: Ortiz de Montellano PR (ed) Cytochrome P450: structure, mechanism, and biochemistry, 3rd edn. Kluwer Academic/Plenum Publishers, New York, pp 183–245
2. Williams JA, Hyland R, Jones BC, Smith DA, Hurst S, Goosen TC, Peterkin V, Koup JR, Ball SE (2004) Drug-drug interactions for UDP-glucuronosyltransferase substrates: a Pharmacokinetic explanation for typically observed low exposure (AUC_i/AUC) ratios. *Drug Metab Dispos* 32:1201–1208
3. Guengerich FP (2008) Cytochrome P450 and chemical toxicology. *Chem Res Toxicol* 21:70–83
4. Schenkman JB, Greim H (eds) (1993) Cytochrome P450, Springer, Berlin
5. Jung C (2011) The mystery of cytochrome P450 compound I: a mini-review dedicated to Klaus Ruckpaul. *Biochim Biophys Acta* 1814:46–57
6. Williams PA, Cosme J, Ward A, Angove HC, Vinkovic DM, Jhoti H (2003) Crystal structure of human cytochrome P450 2C9 with bound warfarin. *Nature* 424:464–468.
7. Williams PA, Cosme J, Vinković DM, Ward A, Angove HC, Day PJ, Vornrhein C, Tickle IJ, Jhoti H (2004) Crystal structures of human cytochrome P450 3A4 bound to metyrapone and progesterone. *Science* 305:683–686
8. Sansen S, Yano JK, Reynald RL, Schoch GA, Griffin KJ, Stout CD, Johnson EF (2007) Adaptations for the oxidation of polycyclic aromatic hydrocarbons exhibited by the structure of human P450 1A2. *J Biol Chem* 282:14348–14355
9. Porubsky PR, Meneely KM, Scott EE (2008) Structures of human cytochrome P-450 2E1. *J Biol Chem* 283:33698–33707
10. Rhiu SY, Ludwig DR, Siu VS, Palmore GTR (2009) Direct electrochemistry of cytochrome P450 27B1 in surfactant films. *Electrochem Commun* 11:1857–1860
11. Newcomb M, Zhang R, Chandrasena REP, Halgrimson JA, Horner JH, Makris TM, Sligar SG (2006) Cytochrome P450 compound I. *J Am Chem Soc* 128:4580–4581
12. Nordblom GD, White RE, Coon MJ (1976) Studies on hydroperoxide-dependent substrate hydroxylation by purified liver microsomal cytochrome P-450. *Arch Biochem Biophys* 175:524–533
13. Rittle J, Green MT (2010) Cytochrome P450 compound I: capture, characterization, and C-H bond activation kinetics. *Science* 330:933–937
14. Vincent KA, Parkin A, Armstrong FA (2007) Investigating and exploiting the electrocatalytic properties of hydrogenases. *Chem Rev* 107:4366–4413
15. Armstrong FA (1997) In: Lenz G, Milazzo G (eds) *Bioelectrochemistry of biomacromolecules*. Birkhauser Verlag, Basel, pp 205–255
16. Rusling JF, Zhang Z (2002) In: Chambers JQ, Brajter-Toth A (eds) *Electroanalytical methods for biological materials*. Marcel Dekker, New York, pp 195–231
17. Rusling JF, Zhang Z (2001) In: Nalwa RW (ed) *Handbook of surfaces and interfaces of materials: biomolecules, biointerfaces, and applications*, vol 5. Academic Press, Cambridge, pp 33–71
18. Bowden EF, Hawkrigde FM, Blount HN (1985) In: Srinivasan S, Chizmadzhev YA, Bockris JO'M, Conway BE, Yeager E (eds) *Comprehensive treatise of electrochemistry*, vol 10. Plenum, New York, pp 297–346

19. Armstrong FA (1990) In: Bioinorganic chemistry: structure and bonding. Springer, Berlin, pp 137–221
20. Yeh P, Kuwana T (1997) Reversible electrode reaction of cytochrome c. *Chem Lett* 6:1145–1148
21. Eddowes MJ, Hill HAO (1977) Novel method for the investigation of the electrochemistry of metalloproteins: cytochrome c. *J Chem Soc Chem Commun* 21:771–772
22. Armstrong FA, Hill HAO, Walton NJ (1988) Direct electrochemistry of redox proteins. *Acc Chem Res* 21:407–413
23. Faulkner KM, Shet MS, Fisher CW, Estabrook RW (1995) Electrocatalytically driven omega-hydroxylation of fatty acids using cytochrome P450 4A1. *Proc Nat Acad Sci USA* 92:7705–7709
24. Estabrook RW, Faulkner KM, Shet MS, Fisher CW (1996) Application of electrochemistry for P450-catalyzed reactions. *Methods Enzymol* 272:44–50
25. Vilker VL, Kahn F, Shen D, Baizer MM, Nobe K (1988) In: Dryhurst G, Niki K (ed) Redox chemistry and interfacial behavior of biological molecules. Plenum, New York, pp 105–112
26. Udit AK, Arnold FH, Gray HB (2004) *J Inorg Biochem* 98:1547–1550
27. Zilly FE, Taglieber A, Schulz F, Hollmann F, Reetz MT (2009) Deazaflavins as mediators in light-driven cytochrome P450 catalyzed hydroxylations. *Chem Commun* 46:7152–7154
28. Kazlauskaitė J, Westlake ACG, Wong L-L, Hill HAO (1996) Direct electrochemistry of cytochrome P450cam. *Chem Commun* 18:2189–2190
29. Rusling JF, Zhang Z (2003) In: Rusling JF (ed) Biomolecular films, Marcel Dekker, New York, pp 1–64
30. Rusling JF, Wang B, Yun SE (2008) In Bartlett PN (ed) Bioelectrochemistry, John Wiley, New York, pp 39–86
31. Yang M, Kabulski JL, Wollenberg L, Chen X, Subramanian M, Tracy TS, Lederman D, Gannett PM, Wu N (2009) Electrocatalytic drug metabolism by CYP2C9 bonded to a self-assembled monolayer-modified electrode. *Drug Metab Dispos* 37:892–899
32. Todorovic S, Jung C, Hildebrandt P, Murgida DH (2006) Conformational transitions and redox potential shifts of cytochrome P450 induced by immobilization. *J Biol Inorg Chem* 11:119–127
33. Ferrero VEV, Andolfi L, Nardo GD, Sadeghi SJ, Fantuzzi A, Cannistraro S, Gilardi G (2008) Protein and electrode engineering for the covalent immobilization of P450 bmp on gold. *Anal Chem* 80:8438–8446
34. Fantuzzi A, Fairhead M, Gilardi G (2004) Direct electrochemistry of immobilized human cytochrome P450 2E1. *J Am Chem Soc* 126:5040–5041
35. Tanvir S, Pantigny J, Boulnois P, Pulvin S (2009) Covalent immobilization of recombinant human cytochrome CYP2E1 and glucose-6-phosphate dehydrogenase in alumina membrane for drug screening applications. *J Membr Sci* 329:85–90
36. Zhang Z, Nassar A-EF, Lu Z, Schenkman JB, Rusling JF (1997) Direct electron injection from electrodes to cytochrome P450 cam in biomembrane-like films. *J Chem Soc Faraday Trans* 93:1769–1774
37. Lvov YM, Lu Z, Schenkman JB, Zu X, Rusling JF (1998) Direct electrochemistry of myoglobin and cytochrome P450 cam in alternate layer-by-layer films with DNA and other polyions. *J Am Chem Soc* 120:4073–4080
38. Zu X, Lu Z, Zhang Z, Schenkman JB, Rusling JF (1999) Electroenzyme-catalyzed oxidation of styrene and cis- β -methylstyrene using thin films of cytochrome P450 cam and myoglobin. *Langmuir* 15:7372–7377
39. Munge B, Estavillo C, Schenkman JB, Rusling JF (2003) Optimization of electrochemical and peroxide-driven oxidation of styrene with ultrathin polyion films containing cytochrome P450 cam and myoglobin. *Chem Bio Chem* 4:82–89
40. Estavillo C, Lu Z, Jansson I, Schenkman JB, Rusling JF (2003) Epoxidation of styrene by human cyt P450 1A2 by thin film electrolysis and peroxide activation compared to solution reactions. *Biophys Chem* 104:291–296

41. Krishnan S, Schenkman JB, Rusling JF (2011) Bioelectronic delivery of electrons to cytochrome P450 enzymes. *J Phys Chem B* 115:8371–8380
42. Bistolas N, Wollenberger U, Jung C, Scheller FW (2005) Cytochrome P450 biosensors-a review. *Biosens Bioelec* 20:2408–2423
43. Krishnan S, Rusling JF (2013) Thin iron heme enzyme films on electrodes and nanoparticles for biocatalysis. In: S. Suib (ed) *New and future developments in catalysis*. Elsevier Publishers, Amsterdam, p. 125
44. Fleming BD, Johnson DL, Bond AM, Martin LL (2006) Recent progress in cytochrome P450 enzyme electrochemistry. *Expert Opin Drug Metab Toxicol* 2:581–589
45. Schneider E, Clark DS (2013) Cytochrome P450 (CYP) enzymes and the development of CYP biosensors. *Biosens Bioelec* 39:1–13
46. Dodhia VR, Gildardi G (2009) In: Davis J (ed) *Engineering the bioelectronic interface: applications to analyte biosensing and protein detection*. RSC publications, London, pp 153–189
47. Krishnan S, Abeykoon A, Schenkman JB, Rusling JF (2009) Control of electrochemical and ferrioxo formation kinetics of cyt P450s in polyion films by heme iron spin state and secondary structure. *J Am Chem Soc* 131:16215–16224
48. Bard A, Faulkner LR (2000) *Electrochemical methods: fundamentals and applications*, 2nd edn. Wiley, New Jersey
49. Heering HA, Hirst J, Armstrong FA (1998) Interpreting the catalytic voltammetry of electroactive enzymes adsorbed on electrodes. *J Phys Chem B* 102:6889–6902
50. Guto PM, Rusling JF (2005) Enzyme-like kinetics of ferrioxo myoglobin formation in films on electrodes in microemulsions. *J Phys Chem B* 109:24457–24464
51. Omura T, Sato R (1964) The carbon monoxide-binding pigment of liver microsomes. *J Biol Chem* 239:2379–2385
52. Sandhu P, Guo Z, Baba T, Martin MV, Tukey RH, Guengerich FP (1994) Expression of modified human cytochrome P450 1A2 in *Escherichia coli*: stabilization, purification, spectral characterization, and catalytic activities of the enzyme. *Arch Biochem Biophys* 309:168–177
53. Sligar SG, Gunsalus IC (1976) A thermodynamic model of regulation: modulation of redox equilibria in camphor monooxygenase. *Proc Natl Acad Sci USA* 73:1078–1082
54. Das A, Grinkova YV, Sligar SG (2007) Redox potential control by drug binding to cytochrome P450 3A4. *J Am Chem Soc* 129:13778–13779
55. Sligar SG (1976) Coupling of spin, substrate, and redox equilibria in cytochrome P450. *Biochemistry* 15:5399–5406
56. Johnson DL, Conley AJ, Martin LL (2006) Direct electrochemistry of human, bovine and porcine cytochrome P450c17. *J Mol Endocrinol* 36:349–359
57. Iwuoha EI, Kane S, Ania CO, Smyth MR, Ortiz de Montellano PR, Fuhr U (2000) Reactivities of organic phase biosensors 3: electrochemical study of cytochrome P450 cam immobilised in a methyltriethoxysilane sol-gel. *Electroanalysis* 12:980–986
58. Lei C, Wollenberger U, Jung C, Scheller FW (2000) Clay-bridged electron transfer between cytochrome P450 cam and electrode. *Biochem Biophys Res Commun* 268:740–744
59. Joseph S, Rusling JF, Lvov YM, Friedberg T, Fuhr U (2003) An amperometric biosensor with human CYP3A4 as a novel drug screening tool. *Biochem Pharmacol* 65:1817–1826
60. Feng D, Schultz FA (1988) Relationship between structural change and heterogeneous electron-transfer rate constant in iron-tetraphenylporphyrin complexes. *Inorg Chem* 27: 2144–2149
61. Cirino PC, Arnold FH (2003) A self-sufficient peroxide-driven hydroxylation biocatalyst. *Angew Chem Int Ed* 42:3299–3301
62. Reipa V, Mayhew MP, Vilker VL (1997) A direct electrode-driven P450 cycle for biocatalysis. *Proc Natl Acad Sci USA* 94:13554–13558
63. Paternolli C, Antonini M, Ghisellini P, Nicolini C (2004) Recombinant cytochrome p450 immobilization for biosensor applications. *Langmuir* 20:11706–11712

64. Liu S, Peng L, Yang X, Wu Y, He L (2008) Electrochemistry of cytochrome P450 enzyme on nanoparticle-containing membrane-coated electrode and its applications for drug sensing. *Anal Biochem* 375:209–216
65. Dai C, Ding Y, Li M, Fei J (2012) Direct electrochemistry of cytochrome P450 in a biocompatible film composed of an epoxy polymer and acetylene black. *Microchim Acta* 176:397–404
66. Sun P, Wu Y (2013) An amperometric biosensor based on human cytochrome P450 2C9 in polyacrylamide hydrogel films for bisphenol A determination. *Sens Actuators B* 178:113–118
67. Wasalathanthri DP, Li D, Song D, Zheng Z, Choudhary D, Jansson I, Lu X, Schenkman JB, Rusling JF (2015) Elucidating organ-specific metabolic toxicity chemistry from Electrochemiluminescent Enzyme/DNA arrays and bioreactor BeadLC-MS/MS. *Chem Sci* 6:2457–2468
68. Hvastkovs EG, So M, Krishnan S, Bajrami B, Tarun M, Jansson I, Schenkman JB, Rusling JF (2007) Electrochemiluminescent arrays for cytochrome P450-activated genotoxicity screening. DNA damage from Benzo[a]pyrene Metabolites. *Anal Chem* 79:1897–1906
69. Krishnan S, Hvastkovs EG, Bajrami B, Choudhary D, Schenkman JB, Rusling JF (2008) Synergistic metabolic toxicity screening using Microsome/DNA Electrochemiluminescent arrays and nanoreactors. *Anal Chem* 80:5279–5285
70. Wasalathanthri DP, Malla S, Bist I, Tang CK, Faria RC, Rusling JF (2013) High-throughput metabolic genotoxicity screening with a fluidic microwell chip and electrochemiluminescence. *Lab Chip* 13:4554–4562
71. Krishnan S, Wasalathanthri D, Zhao L, Schenkman JB, Rusling JF (2011) Efficient bioelectronic actuation of the natural catalytic pathway of human metabolic cytochrome P450s. *J Am Chem Soc* 133:1459–1465
72. Dodhia VR, Sassone C, Fantuzzi A, Nardo GD, Sadeghi SJ, Gilardi G (2008) Modulating the coupling efficiency of human cytochrome P450 CYP3A4 at electrode surfaces through protein engineering. *Electrochem Commun* 10:1744–1747
73. Walgama C, Nerimetla R, Materer NF, Schildkraut D, Elman JF, Krishnan S (2015) A simple construction of electrochemical liver microsomal bioreactor for rapid drug metabolism and inhibition assays. *Anal Chem* 87:4712–4718
74. Sultana N, Schenkman JB, Rusling JF (2005) Protein film electrochemistry of microsomes genetically enriched in human cytochrome P450 monooxygenases. *J Am Chem Soc* 127:13460–13461
75. Mie Y, Suzuki M, Komatsu Y (2009) Electrochemically driven drug metabolism by membranes containing human cytochrome P450. *J Am Chem Soc* 131:6646–6647
76. Bajrami B, Krishnan S, Rusling JF (2008) Microsome biocolloids for rapid drug metabolism and inhibition assessment by LC-MS. *Drug Metab Lett* 2:158–162
77. Rudakov YO, Shumyantseva VV, Bulko TV, Suprun EV, Kuznetsova GP, Samenkova NF, Archakov AI (2008) Stoichiometry of electrocatalytic cycle of cytochrome P450 2B4. *J Inorg Biochem* 102:2020–2025
78. Chatterjee S, Sengupta K, Samanta S, Kumar Das P, Dey A (2013) Electrocatalytic O₂ reduction reaction by synthetic analogues of cytochrome P450 and myoglobin: in-situ resonance raman and dynamic electrochemistry investigations. *Inorg Chem* 52:9897–9907
79. Wong A, de Vasconcelos Lanza MR, Sotomayor MDPT (2013) Sensor for diuron quantitation based on the P450 biomimetic catalyst nickel(II) 1,4,8,11,15,18,22,25-octabutoxy-29H,31H-phthalocyanine. *J Electroanal Chem* 690:83–88
80. da Silva DC, De Freitas-Silva G, do Nascimento E, Rebouças JS, Barbeira PJS, Dai de Carvalho MEM, Idemori YM (2008) Spectral, electrochemical, and catalytic properties of a homologous series of manganese porphyrins as cytochrome P450 model: the effect of the degree of β -bromination. *J Inorg Biochem* 102:1932–1941

Electrochemistry of N4 Macrocyclic Metal Complexes

Volume 2: Biomimesis, Electroanalysis and

Electrosynthesis of MN4 Metal Complexes

Zagal, J.H.; Bedioui, F. (Eds.)

2016, XV, 436 p. 263 illus., 159 illus. in color.,

Hardcover

ISBN: 978-3-319-31330-6